Global network of slow solar wind

N. U. Crooker,[1] S. K. Antiochos,[2] X. Zhao,[3] and M. Neugebauer[4]

Received 5 October 2011; revised 18 January 2012; accepted 18 February 2012; published 6 April 2012.

[1] The streamer belt region surrounding the heliospheric current sheet (HCS) is generally treated as the primary or sole source of the slow solar wind. Synoptic maps of solar wind speed predicted by the Wang-Sheeley-Arge model during selected periods of solar cycle 23, however, show many areas of slow wind displaced from the streamer belt. These areas commonly have the form of an arc that is connected to the streamer belt at both ends. The arcs mark the boundaries between fields emanating from different coronal holes of the same polarity and thus trace the paths of belts of pseudostreamers, i.e., unipolar streamers that form over double arcades and lack current sheets. The arc pattern is consistent with the predicted topological mapping of the narrow open corridor or singular separator line that must connect the holes and, thus, consistent with the separatrix-web model of the slow solar wind. Near solar maximum, pseudostreamer belts stray far from the HCS-associated streamer belt and, together with it, form a global-wide web of slow wind. Recognition of pseudostreamer belts as prominent sources of slow wind provides a new template for understanding solar wind stream structure, especially near solar maximum.

Citation: Crooker, N. U., S. K. Antiochos, X. Zhao, and M. Neugebauer (2012), Global network of slow solar wind, *J. Geophys. Res.*, *117*, A04104, doi:10.1029/2011JA017236.

1. Introduction

[2] In the 1970s, two factors fostered a major advance in our understanding of the pattern of fast and slow wind measured in the ecliptic plane at 1 AU. These were the advent of continuous X-ray observations of the Sun taken from Skylab combined with a remarkably well-ordered, dipole-dominated configuration of the solar magnetic field during the declining phase of solar cycle 20, especially in 1974. The X-ray observations revealed large polar coronal holes centered on a dipolar axis tilted with respect to the heliographic equator. *Hundhausen* [1977] was quick to deduce that under this configuration the Sun's rotation would bring alternating streams of fast wind to the ecliptic plane, one with positive polarity from the northern coronal hole and one with negative polarity from the southern hole, separated by slow wind from the streamer belt sandwiched between the holes, as observed. The slow wind thus forms a band encompassing the heliospheric current sheet (HCS), which stems from the heliomagnetic equator threading the tilted streamer belt.

[3] In the ensuing years this tilted dipole pattern with its band of slow wind became an indelible template for organizing solar wind studies. From the heliospheric point of view, based primarily upon the ever-present magnetic sector structure, variations during the course of the solar cycle were nominally understood in terms of a rotation of the dipole axis from alignment with the spin axis at solar minimum to an orthogonal orientation at solar maximum, on its way toward a full reversal of the Sun's polarity at the next minimum, although what physical process could account for such an apparent rotation was left as an open question. What the template does not address, however, is evidence that the slow wind is considerably more widespread than the template allows. This is particularly true at solar maximum, when nearly all semblance of an orderly solar wind flow pattern seems to disappear, save for the sector structure. This "chaos" [*McComas et al.*, 2002] has traditionally been ascribed to the replacement of large polar coronal holes with a random pattern of small, low-latitude coronal holes that form near active regions [e.g., *Wang and Sheeley*, 2003]. Evidence for widespread slow wind was also present during the recent extended solar minimum. One way to accommodate it is to assume that the band of slow wind surrounding the HCS is considerably broader than the width of the streamer material, as suggested by *Zhao and Fisk* [2010], building upon their model of slow wind release from coronal loops through interchange reconnection with open flux [e.g., *Fisk et al.*, 1998; *Fisk and Schwadron*, 2001; *Fisk*, 2005]. *Antiochos et al.* [2011, 2012] propose an alternative way to broaden the band of slow wind at solar minimum. They assume the same method of slow wind release, but the release occurs along discrete bands that branch off from the HCS and form a broad network of slow wind outflow. Here we follow the lead of *Antiochos et al.* [2011, 2012] and demonstrate further that, near solar maximum, the network

[1]Center for Space Physics, Boston University, Boston, Massachusetts, USA.
[2]NASA Goddard Space Flight Center, Greenbelt, Maryland, USA.
[3]W. W. Hansen Experimental Physics Laboratory, Stanford University, Stanford, California, USA.
[4]Lunar and Planetary Laboratory, University of Arizona, Tuscon, Arizona, USA.

0148-0227/12/2011JA017236

of discrete bands expands to cover the entire sphere of the source surface. The tilted dipole template is preserved within this structure because the network includes the band of slow wind surrounding the HCS, which, in itself, does not broaden.

[4] We begin with an analysis of the relatively confined configuration of the slow wind during the recent solar minimum period addressed by *Antiochos et al.* [2011, 2012] and then move on to an analysis of the global-wide configuration at the beginning of the preceding declining phase of the solar cycle. Discussion and conclusions follow.

2. Analysis

[5] Two tools are used for analysis. The first is the Wang-Sheeley-Arge (WSA) model [e.g., *Arge et al.*, 2004] for predicting solar wind speed. The Community Coordinated Modeling Center has provided synoptic maps of predicted speed at a distance of 5 R_S from the Sun based upon magnetograms from the Mount Wilson Observatory. Although the WSA model has only been tested against observations in the ecliptic plane, we base our analysis upon an assumed validity of the model across high latitudes, as well. The second tool is a set of potential field source surface (PFSS) maps based upon MDI magnetograms from the SOHO spacecraft. These were designed to trace boundaries between open field lines from different coronal holes and were first used by *Zhao and Webb* [2003] to identify source regions of coronal mass ejections. We note that the two tools are not independent of each other, since the WSA model is also based upon PFSS calculations. Their purpose is only to provide both field and flow views of the slow wind patterns. In addition, the analysis uses plasma [*McComas et al.*, 1998], ionic composition [*Gloeckler et al.*, 1998], and magnetic field data [*Smith et al.*, 1998] from the Advanced Composition Explorer (ACE) spacecraft located in the ecliptic plane near 1 AU.

2.1. Solar Minimum

[6] We select Carrington Rotation (CR) 2072 for our analysis, which covers 7 July to 3 August 2008 during the recent deep solar minimum. Extensive modeling of the Sun's magnetic configuration during this rotation was performed by Predictive Science, Inc., in preparation for predictions for the solar eclipse on 1 August 2008 [*Rusin et al.*, 2010], and the modeling results formed the basis of much of the analysis by *Antiochos et al.* [2011, 2012], upon which we wish to build.

[7] Figure 1a shows a synoptic map of the distribution of solar wind speed at 5 R_S predicted by the WSA model for this rotation. As expected, the heavy blue band of slow wind traces the path of the HCS, which, at this phase of the solar cycle, lies close to the heliographic equator. What is unexpected is the splitting of the slow wind into a double band on the right side of Figure 1, between Carrington longitudes 240° and 360°, where the latitudinal distance between the bands reaches 40°. The HCS, however, does not split. It threads the lower band, which carries the slowest wind. Although the split has not been verified by observations, we shall assume that the model pattern is real and deduce its properties.

[8] If we describe the upper band of the split slow wind pattern in Figure 1a as an arc of slow wind attached to the streamer belt at both ends, it is easy to recognize it as the pattern predicted by *Antiochos et al.* [2011] (their Figure 1) for the heliospheric mapping of a narrow corridor of open field lines connecting a low-latitude coronal hole to the polar coronal hole of the same polarity. This configuration is apparent in the PFSS map of open field line regions on the Sun's surface in Figure 2a, which shows a V-shaped coronal hole in the same longitude range as the split slow-wind pattern, lying north of the heliomagnetic equator but south of the northern polar coronal hole and lying in the same (negative) magnetic polarity region as the polar hole. (Note that the sin (latitude) plotted as the ordinate in Figures 2a and 2b exaggerates the extent of low-latitude features.) Although the required corridor (or separator line—see section 3) between the holes cannot be seen at this resolution, its mapping to the heliosphere as an arc of slow wind seems undeniable. If the V-shaped coronal hole were truly disconnected from the polar hole, its mapping to the heliosphere would not connect to the HCS [*Antiochos et al.*, 2007, 2011].

[9] A more intuitive way to view the arc of slow wind is shown in the PFSS map of open field line regions on the source surface (at 2.5 R_S) in Figure 2c, where the different colors indicate lines from different coronal holes and the encircled points outline the boundaries between them. Here the arc clearly forms the boundary between red open field lines from the polar coronal hole and magenta and cyan field lines from the two branches of the V comprising the low-latitude coronal hole. Similar mappings can be found in the work of *Wang and Sheeley* [1990b] and *Wang et al.* [2009]. *Zhao and Webb* [2003] call this kind of arc a "unipolar boundary," distinguishing it from the "bipolar boundary" at the HCS. Here we identify unipolar boundaries with heliospheric mappings of corridors or separator lines between coronal holes. Figure 2c also shows unipolar boundaries associated with the low-latitude coronal holes south of the heliomagnetic equator. These are discussed at the end of this section.

[10] Figure 2b provides a guide for picturing the magnetic configuration surrounding the arc of slow wind. It shows the closed magnetic loops immediately underlying the open fields from the coronal holes, color-coded accordingly. For example, the familiar configuration of the helmet streamer belt can be seen in the longitude range 0° to 150°. There the loops are half red and half blue to match the overlying open fields from the north (red) and south (blue) polar coronal holes. The color change from red to blue occurs at the apex of each loop, where it arches over the heliomagnetic equator, at the base of the HCS. (The gaps between the red and blue sides are artifacts of the large grid size.) In the longitude range of the low-speed arc, ~240° to 360°, the configuration changes. The portion of the helmet streamer belt on the north side of the heliomagnetic equator is now formed by the magenta and cyan loops that fan out southward from points adjacent to the low-latitude coronal hole. Those that fan out northward comprise one of two sets of uniformly colored loops that form the base of what has been named a "pseudostreamer" by *Wang et al.* [2007] or, alternatively, a "unipolar streamer" by *Riley and Luhmann* [2012]. (The more familiar cross-section of a pseudostreamer can be seen on the east limb in Figure 3, discussed below.) The second set of loops at the base of the pseudostreamer is the array of red

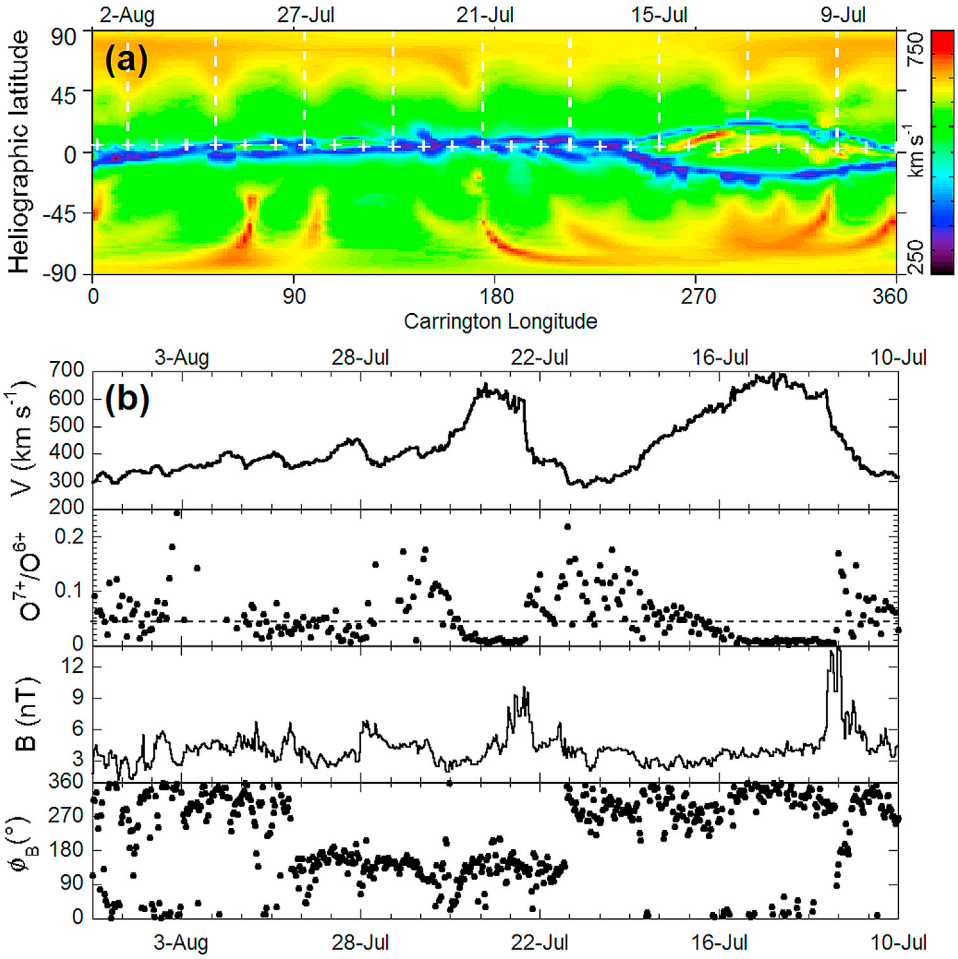

Figure 1. (a) Color-coded synoptic map of the solar wind speed distribution at 5 R_S for CR 2072 predicted by the Wang-Sheeley-Arge model based upon solar magnetograms from the Mount Wilson Observatory. Plus signs mark intersection with the ecliptic plane. (b) ACE spacecraft measurements of solar wind speed V, oxygen charge-state ratio O^{7+}/O^{6+}, magnetic field magnitude B and longitude ϕ_B (GSE coordinates), lagged by 3 days and plotted backward in time to match features in Figure 1a.

loops lying under open field lines from the northern coronal hole. Their equatorward foot points outline the unipolar boundary marking the arc of slow wind, as seen in Figure 2c. The slow wind can thus be said to arise from a pseudostreamer belt. Any open field lines in a narrow corridor (or corridors) between the polar and low-latitude coronal holes presumably rise from some path among the red, magenta, and cyan loops at the base of the pseudostreamer and then splay out to fill the space between the field lines from the two coronal hole sources, as pictured by *Antiochos et al.* [2011, 2012].

[11] The pseudostreamer structure is best seen in cross section in the MHD model of the solar configuration in Figure 3 generated by *Rusin et al.* [2010] for the eclipse predictions mentioned above, where the longitude of the east limb, ~290°, passes through the heart of the double band of slow wind. As these authors note, the structure in the northern hemisphere on the east limb is a pseudostreamer. In contrast to the helmet streamer in the southern hemisphere on the east limb, the pseudostreamer has two loops rather than one loop at its base. The outer legs of both loops have negative polarity, as do the overlying open field lines from the polar and low-latitude coronal holes. Consequently there is no heliospheric current sheet in the pseudostreamer, as is apparent in Figure 1a, where the arc of slow wind lacks a current sheet, as discussed above.

[12] It is clear from the magnetic configuration on the east limb in Figure 3 that the double band of slow wind from the streamer and pseudostreamer is a global-scale structure rather than some substructure in the streamer belt. Data from the ecliptic plane at 1 AU support this view. The resulting, well-formed stream structure is shown in Figure 1b, where the data are plotted backward in time and lagged by 3 days in order to approximately align with features near the Sun in Figure 1a and Figure 2. The low-latitude coronal hole between the streamer and pseudostreamer is the source of a high-speed stream, with winds approaching 700 k s^{-1} on 14 July. An additional, narrower high-speed stream peaking near 650 k s^{-1} on 23 July has its source in the set of low-latitude coronal holes in the southern hemisphere centered near 200° longitude, consistent with the change in magnetic polarity on 21 July, plotted in the bottom panel of Figure 1b.

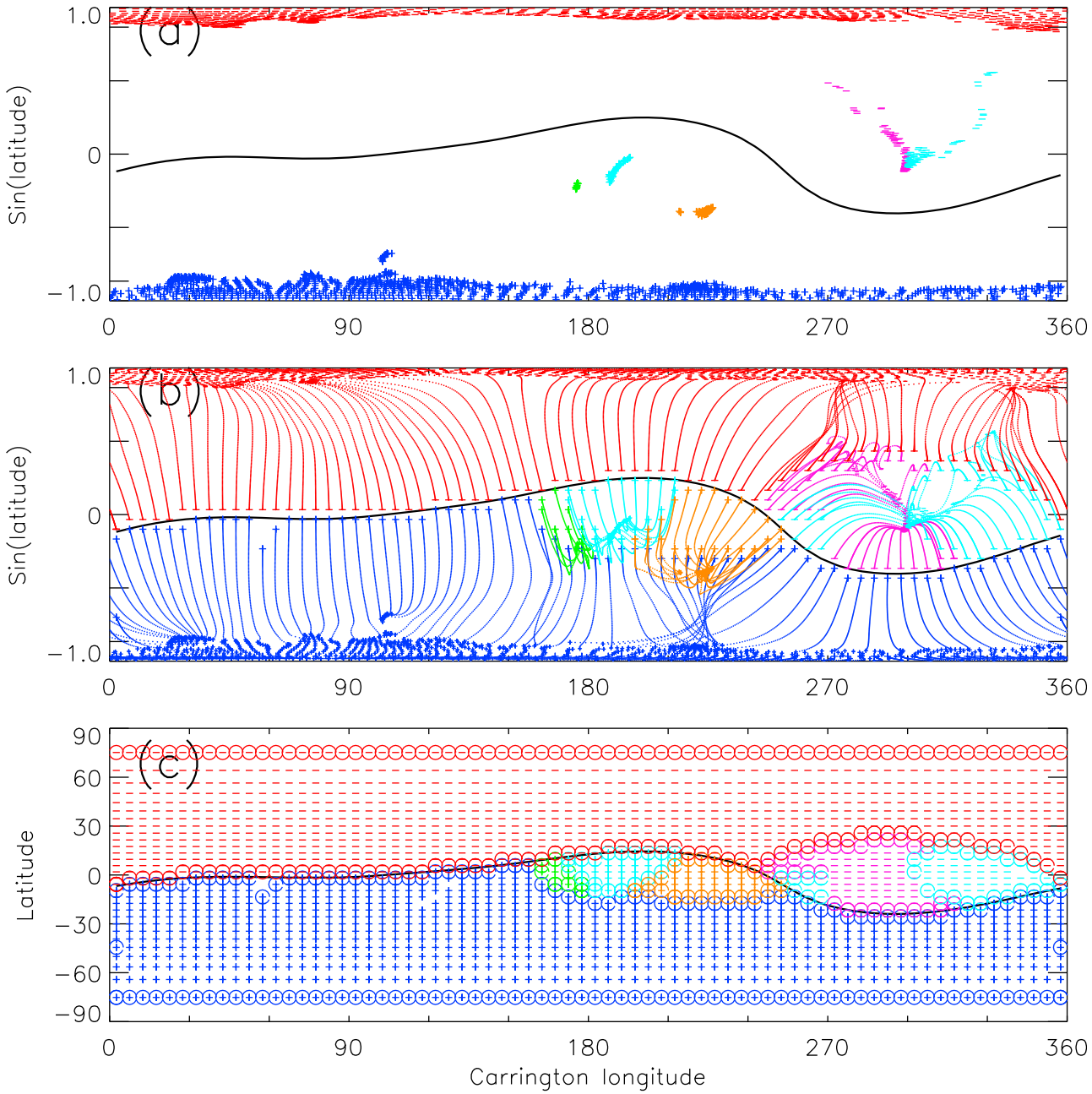

Figure 2. Color-coded potential field source surface model maps for CR 2072 calculated from MDI magnetograms: (a) foot points of open field lines in coronal holes at 1 R_S, (b) closed field lines immediately beneath the open field lines between 1 R_S and the source surface at 2.5 R_S, and (c) open field lines at the source surface, where the circled points outline the boundaries between flux from different coronal holes.

Although the corresponding arc of slow wind stemming southward from the streamer belt is not apparent in Figure 1a, the unipolar boundary indicating its presence can be seen in cyan and orange in Figure 2c.

[13] Both streams in Figure 1b create preceding interaction regions of compression indicated by the peaks in magnetic field magnitude on 12 July and 22 July in the third panel of Figure 1b. The interaction regions contain stream interfaces between what was originally fast and slow wind, and these are marked by sharp changes in the oxygen charge state ratio plotted in the second panel (cf. N. U. Crooker and R. L. McPherron, Coincidence of composition and speed boundaries of the slow solar wind, submitted to the *Journal of Geophysical Research*, 2012). The plot clearly shows that the ratio within the high-speed flows was well below the dashed horizontal line at 0.045, indicating a coronal hole origin [e.g., *Zhao and Fisk*, 2010].

[14] In summary, models and data from CR 2072 during the recent, deep solar minimum indicate that slow wind was not completely confined to a near-equatorial streamer belt,

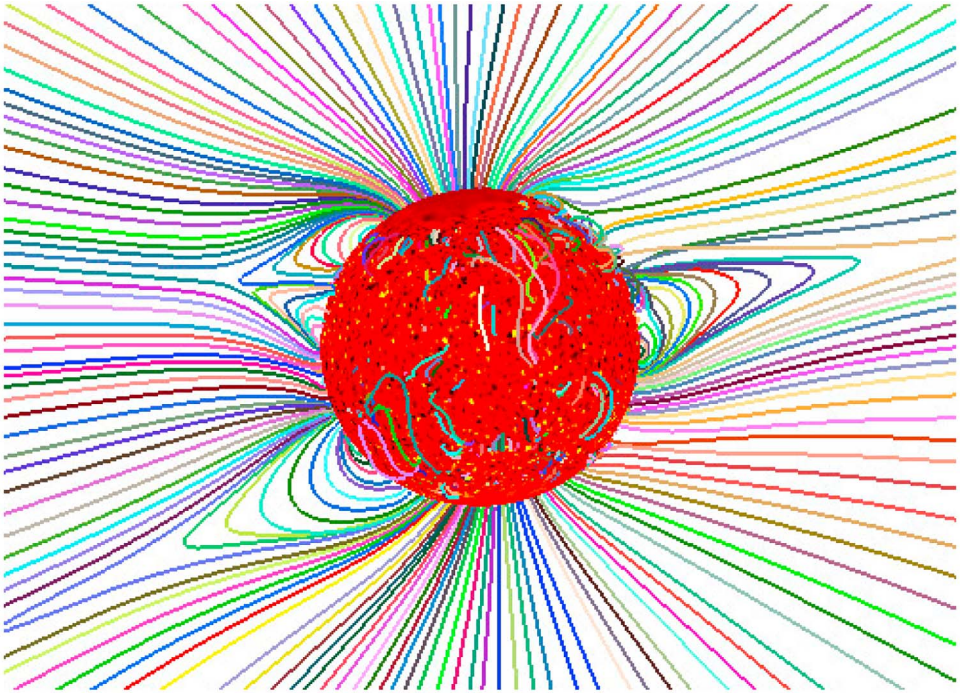

Figure 3. MHD model magnetic field lines for CR 2072, where the configuration on the east limb in the northern hemisphere shows the pseudostreamer at Carrington longitude 290° in cross-section [from *Rusin et al.*, 2010].

as might be expected. Instead, in a limited longitude range, a band of slow wind split off from the streamer belt, forming an arc with its apex 40° removed from the streamer belt. This kind of pattern was predicted by *Antiochos et al.* [2011, 2012] for the heliospheric mapping of open-field corridors connecting polar and low-latitude coronal holes. A PFSS model indicates that the arc traced a unipolar boundary between fields from separate coronal holes. These open fields converged over double loops to form a pseudostreamer structure that gave rise to the slow wind in the arc. The global pattern of split slow wind sources was responsible for a pronounced high-speed stream at 1 AU.

2.2. Early Declining Phase

[15] Having learned to recognize an arc of slow solar wind separated from the streamer belt under the relatively simple conditions of solar minimum, we find an abundance of these features in the more complicated patterns near solar maximum. In this section we use the same tools used in section 2.1 to analyze model patterns during CR 1997, which covers 30 November to 27 December 2002, just after solar maximum, at the beginning of the declining phase of cycle 23.

[16] Like Figure 1a, Figure 4a is a synoptic map of the distribution of solar wind speed at 5 R_S predicted by the WSA model for CR 1997. In this case a white curve outlines the HCS in the blue band of slow wind in the streamer belt in order to distinguish it from the many additional areas of slow wind. We focus on the five areas that intersect the ecliptic plane, marked by numbers along the line of white plus signs across the map, in order to compare them with spacecraft data measured near Earth. The data are plotted in Figure 4b, backward in time, as in Figure 1b, and lagged, in this case by 6 days, in order to approximately align with features near the Sun in Figure 4a. (It is not clear why the lag in this case should be twice as long as the 3 day lag applied to CR2072 in Figure 1, given that the solar wind speeds, on average, are roughly the same for both cases. Of course, these lags are approximate, with 5 days being typical, and the line-up of features usually shifts across a map. For example, the 6 day lag applied to Figure 4 results in a misalignment of feature 1, which displays a lag closer to 3 days.)

[17] Of the five numbered areas of slow flow in Figure 4a, only areas 3 and 5 are streamer belt flows encompassing the HCS. Figure 4b (bottom panel) shows the corresponding change in magnetic polarity at these sector boundaries. The remaining three areas connect to the streamer belt at high latitudes but stray far from it in the ecliptic plane. Area 1 has the shape of an arc similar to the one discussed in section 2.1. It matches the unipolar boundary labeled "1" in the PFSS map in Figure 5c, and its magnetic structure is that of a pseudostreamer. The legs of the pseudostreamer are rooted in two low-latitude coronal holes located south of the HCS, colored dark pink/gray and purple in Figure 5a. Figure 5b shows the underlying, correspondingly colored double loop system of the pseudostreamer. Its alignment is nearly orthogonal to the alignment of the pseudostreamer in Figures 2 and 3. Similarly, although area 2 is quite broad in Figure 4a, its western boundary matches a unipolar boundary in Figure 5, and the legs of the corresponding pseudostreamer are rooted in the purple and green low-latitude coronal holes south of the HCS. Area 4 is more structured, with a double dip in speed, but it also matches a unipolar boundary in Figure 5. In this case the legs of the corresponding

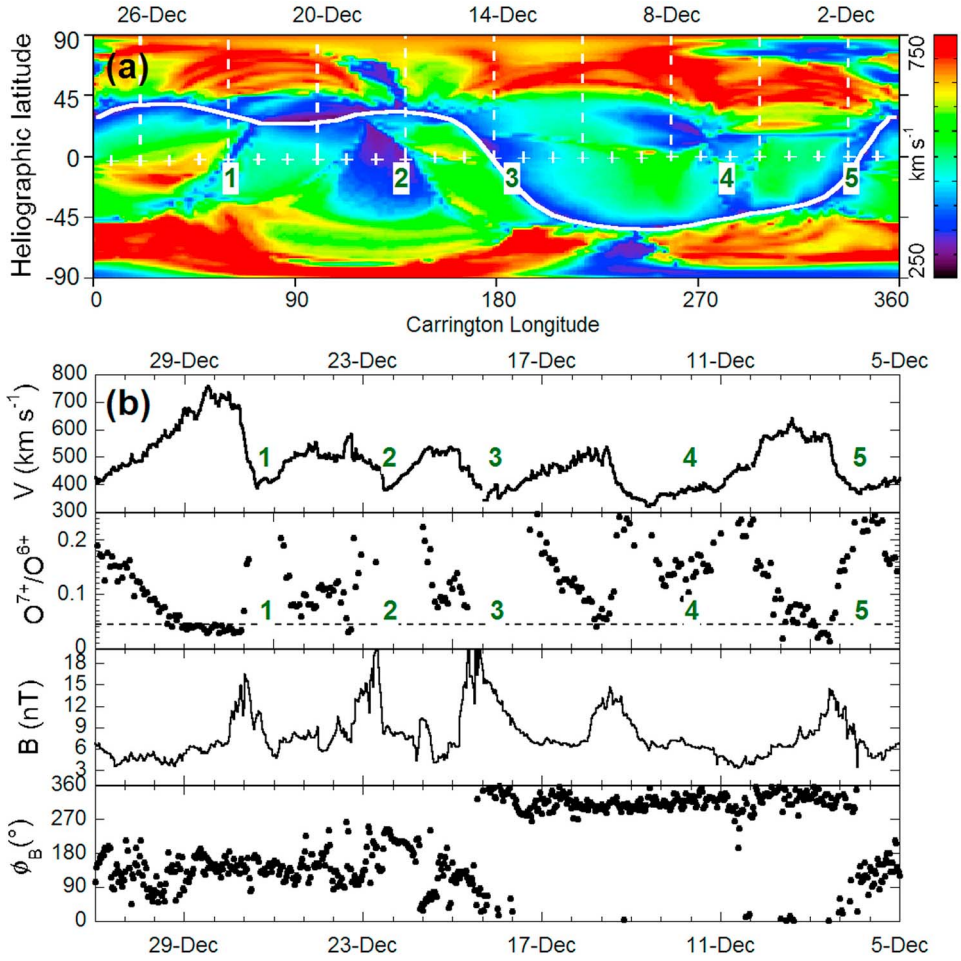

Figure 4. Same as Figure 1 for CR 1997 except that the data are lagged by 6 days. Numbered features identify slow wind in the ecliptic plane.

pseudostreamer are rooted in low-latitude coronal holes north of the HCS, colored magenta and orange.

[18] Figure 4b shows the solar wind stream structure in the ecliptic plane at 1 AU for CR 1997. Although it is more complicated than the pattern at solar minimum in Figure 1b, it clearly matches features in Figure 1a near the Sun. The top panel shows five streams with elevated speed separated by five intervals of low speed corresponding to the five numbered areas in Figure 4a. The oxygen charge state ratio in the second panel follows the expected pattern of high values in the numbered low-speed flows and low values in the faster flows. This well-known anticorrelation [e.g., *Gloeckler et al.*, 2003; *Zurbuchen et al.*, 2002] is particularly notable here because speeds in the three middle streams reach only moderate values, around 500 k s^{-1}, and, accordingly, the charge state ratios barely dip below the 0.045 level typical of coronal hole origin. An exception is the double-dip structure in area 4, which is considerably more pronounced in charge state than in speed.

[19] In the third panel of Figure 4b there are five peaks in the magnetic field magnitude signaling compression in the stream interaction regions generated by the five streams. In the tilted dipole template described in section 1, there are only two streams and, thus, only two interaction regions per solar rotation, and these encompass HCS crossings that precede peak field magnitude. In the case of CR 1997, however, there are three interaction regions in addition to the two that encompass HCS crossings. Cases like these were first analyzed by *Neugebauer et al.* [2004], as reflected in the title of their paper, "Solar wind stream interaction regions without sector boundaries." Here we ascribe them to passage through pseudostreamer belts that form arcs stemming from the streamer belt.

[20] To illustrate the widespread occurrence and evolution of pseudostreamer arcs during the early declining phase of the solar cycle, Figure 6 presents WSA synoptic maps for six successive even-numbered Carrington Rotations beginning with CR 1996, which immediately precedes the map (for CR 1997) in Figure 4a. The HCS (not drawn) threads through all of these maps in much the same form as in Figure 4a, through a blue band of slow flow comprising the streamer belt, but other blue bands of slow flow are pervasive. Because these other bands form arcs that connect to the streamer belt, the combined blue traces in the maps often have the appearance of links in a chain, or a web or network of linked loops. The pattern constantly evolves. Arc 1 in Figure 4a traces the bottom portion of a link that is much more pronounced in the preceding CR 1996 at the top of

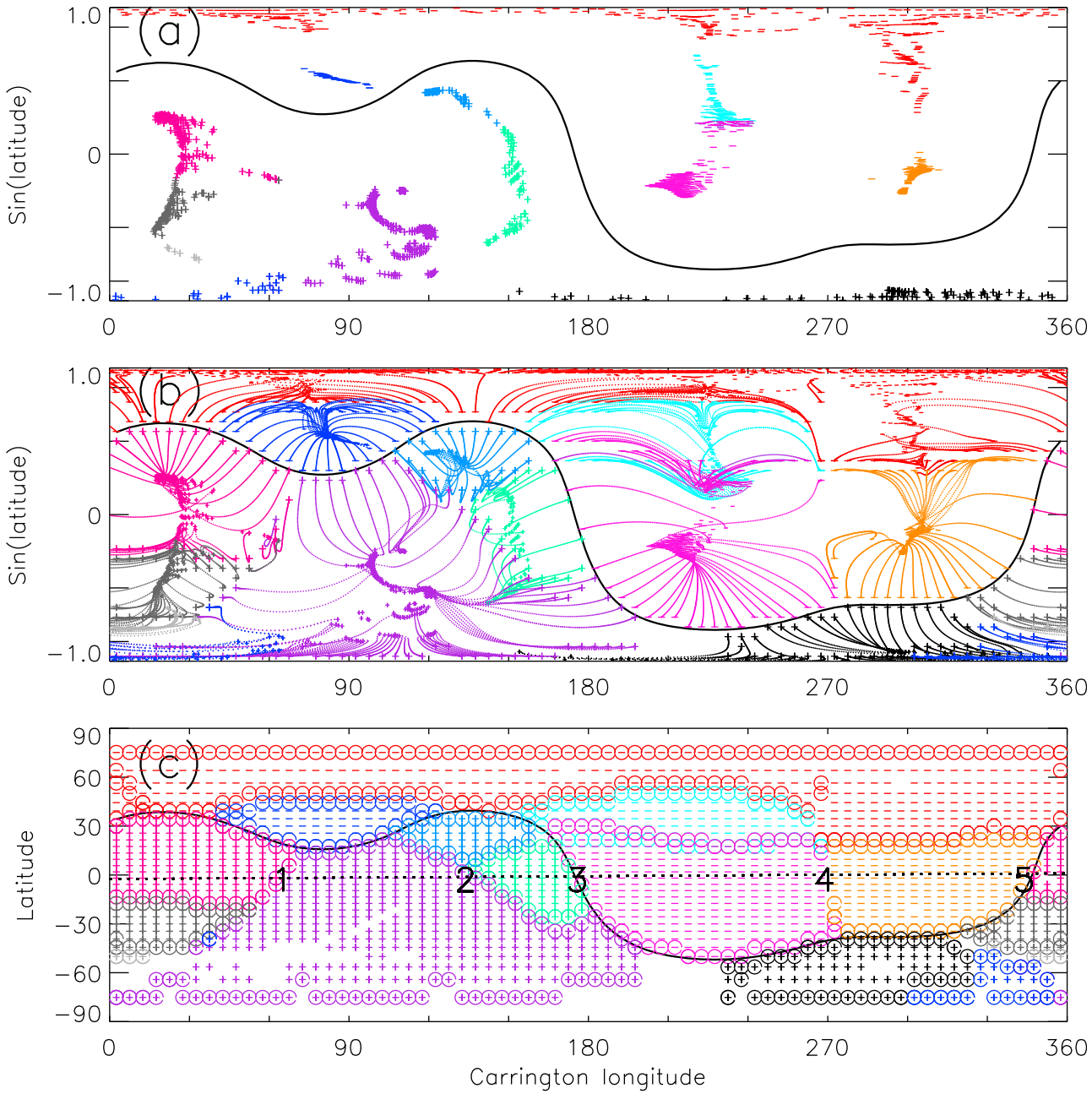

Figure 5. Same as Figure 2 for CR 1997. Numbered boundaries in Figure 5c correspond to numbered features in Figure 4.

Figure 6 but fades away by CR 2002. All that remains in the 0°–180° longitude range is the blue band of the streamer belt. In contrast, in the 180°–360° longitude range, the blue web of slow flow has developed into what looks like a large oval link with two crossbars. By CR 2006, four relatively uniform oval links span the map.

[21] In summary, the complicated solar wind stream structure observed in the ecliptic plane early in the declining phase of the solar cycle can be ascribed to multiple bands of slow wind that are distinct from the slow wind from the streamer belt surrounding crossings of the HCS. Similar to the simpler case analyzed in section 2.1 during solar minimum, the bands of slow wind have pseudostreamer topology characteristic of unipolar boundaries between open fields from different coronal holes. Synoptic maps of predicted speed show that the bands together with the streamer belt form a global network of slow wind that has the appearance of a web of linked loops.

3. Discussion

[22] We begin this section with a brief discussion of relevant aspects of slow solar wind models and then focus on the role of pseudostreamer belts in understanding the global distribution of slow wind. The two leading models for generating slow wind, as reviewed, for example, by *Antiochos*

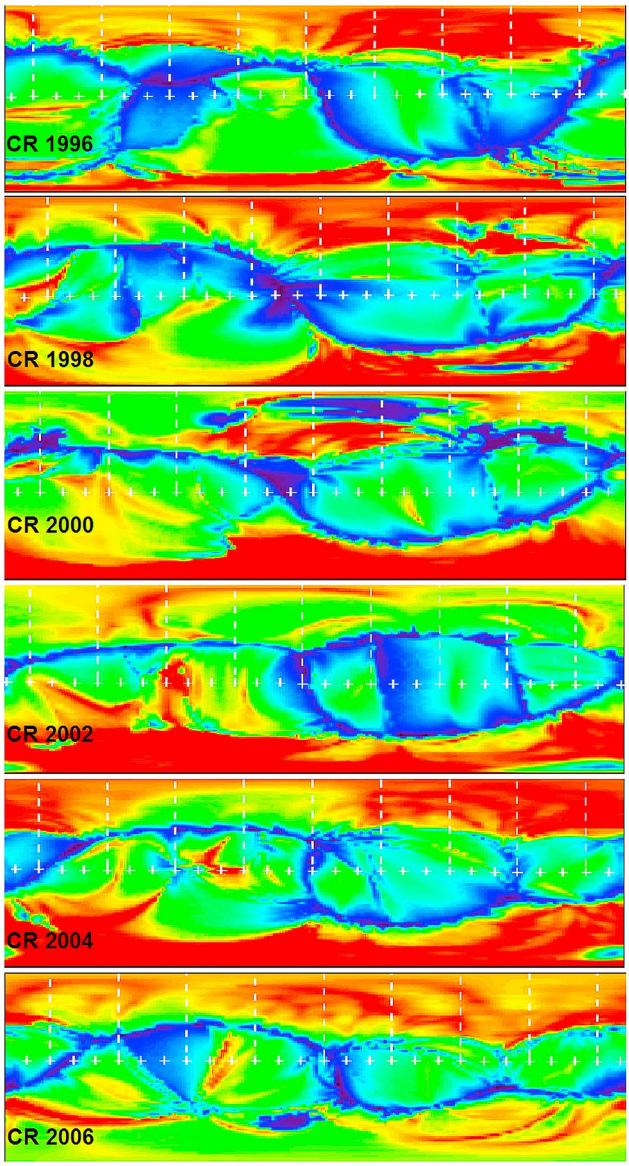

Figure 6. Wang-Sheeley-Arge model predictions for the distribution of solar wind speed at 5 R_S for alternating Carrington Rotations spanning November 2002 through August 2003. Speeds are coded according to the color bar in Figure 1 and Figure 4.

et al. [2011] and *Riley and Luhmann* [2012], are large expansion factors of the magnetic field as it diverges out into the heliosphere [e.g., *Wang and Sheeley*, 1990a], and interchange reconnection between large loops in the streamer belt and open field lines that empties plasma from the newly opened loops into the heliosphere [e.g., *Fisk et al.*, 1998, 1999]. The WSA model used in our analysis essentially incorporates both mechanisms, the latter by adding a factor proportional to distance from the coronal hole boundary [cf. *Riley et al.*, 2001; *Riley and Luhmann*, 2012]. While both mechanisms result in slow wind from the vicinity of the streamer belt, only the interchange reconnection model consistently results in slow wind from pseudostreamer belts. The traditional expansion factor model yields fast wind from pseudostreamer belts [e.g., *Wang and Sheeley*, 1990b; *Wang et al.*, 2007; *Riley and Luhmann*, 2012], although recent developments indicate a range of speeds, from slow to fast, depending upon the height of the cusp (Y.-M. Wang, private communication, 2011). In the WSA model, the factor proportional to distance from the coronal hole boundary clearly dominates its traditional expansion factor, yielding slow flow from pseudostreamer belts, as illustrated in Figures 1, 4, and 6.

[23] The concept of a pseudostreamer belt has been discussed for some time in the literature, although not by that name [e.g., *Eselevich*, 1998; *Eselevich et al.* 1999; *Zhao and Webb*, 2003]. Here, following *Titov et al.* [2011], we propose that pseudostreamer belts are threaded by the quasi- or true separatrix layers of the separatrix-web (S-web) model of the slow solar wind proposed by *Antiochos et al.* [2011, 2012]. Figure 7 schematically illustrates the (quasi-) separatrix layer (dashed curve) in the cross-section of a simple pseudostreamer configuration. We emphasize, however, that the third dimension is critically important for understanding the arcs that appear in the heliosphere, as in Figures 2 and 5. In the simplest and most common situation, Figure 7 would correspond to the magnetic topology of a small negative polarity region wholly embedded in a large-scale positive polarity coronal hole, as in the magnetic field of a plume [e.g., *Wang et al.*, 2007]. For this situation, the dashed lines in Figure 7 correspond to true separatrices and the "X" to a true magnetic null. Although the mapping of these separatrices into the heliosphere does produces a quasi-separatrix layer arc (or point) there, this arc does not connect to the HCS. The arcs shown in Figures 2 and 5, on the other hand, all connect to the HCS, indicating that in the third dimension the open field regions must be connected either by corridors of finite flux [*Antiochos et al.*, 2007, 2011] or by links of singular width [*Titov et al.*, 2011]. In this more general case, the "X" would correspond not to an isolated null point but to a separator line [*Titov et al.*, 2011].

[24] Irrespective of whether the "X" denotes a null or some 3D separator, it invariably locates the site of interchange

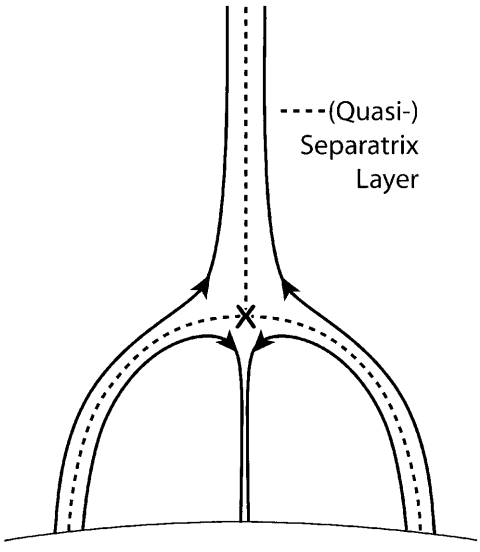

Figure 7. Schematic illustration of the magnetic configuration of a pseudostreamer. "X" marks the site of interchange reconnection between loops and overlying open field lines.

reconnection between the open field lines and the closed loops immediately beneath them. As first noted by *Wang et al.* [2007], although the polarity of the open field lines matches that of the legs of the loops at the photospheric surface, antiparallel components present themselves at the top of the loops. In the S-web model, this interchange reconnection releases plasma from the closed loops to produce the slow wind with its characteristic elemental and charge-state signatures, as proposed by *Fisk* [2003].

[25] Identifying pseudostreamer belts with the (quasi-) separatrix layers of the S-web model affords an explanation for the web-like pattern in the WSA model maps rather than isolated regions of slow wind. As illustrated by *Antiochos et al.* [2011, 2012], the required connection between a polar and low-latitude coronal hole of the same polarity maps out to the heliosphere as an arc of open field lines threaded by a (quasi-) separatrix layer connected at both ends to the HCS, which is a true separatrix layer. It is the connectedness of the separatrices reflecting the required connectedness of the coronal holes (even if only by a separator line) that leads to a web-like pattern of slow flow, with the HCS serving as a backbone for the structure. Alternatively, viewed in the context of the unipolar and bipolar boundaries of *Zhao and Webb* [2003], one can say that the web-like pattern is the natural outcome of bringing together volumes of open flux from multiple coronal holes.

[26] While *Antiochos et al.* [2011] describe the web-like pattern of slow flow primarily in terms of low-latitude substructure surrounding the streamer belt at solar minimum, a key discovery of this work is that the web expands to fill the heliosphere near solar maximum, when the open field pattern on the photosphere appears to consist of a random collection of unrelated coronal holes. We have shown that their mapping to the heliosphere is still well-structured, encompassed by a (quasi-) separatrix web emanating from the HCS. Note in Figure 5 that all of the hole boundaries connect directly to the HCS. *Zhao and Webb* [2003] anticipated the expansion of the web of interconnected pseudostreamer and streamer belts at solar maximum by noting the widespread presence of their equivalent "unipolar coronal streamer belts."

[27] Further, this paper demonstrates that the global network of pseudostreamers and streamers near solar maximum produces recognizable solar wind stream structure in the ecliptic plane that in the past has often been described as lacking any kind of order, especially in contrast to the tilted dipole template described in section 1, with its two streams of opposite polarity per solar rotation. Section 2.2 shows how a considerably more complicated pattern, with five streams in a single rotation, matches the corresponding solar pattern indicating three pseudostreamer belt crossings in addition to the expected two streamer belt crossings. Solar wind data from some of the subsequent solar rotations (not shown) reveal even more complicated stream structure, but these, too, can be understood in terms of a combination of pseudostreamer and streamer crossings, where the difference between them, following *Neugebauer et al.* [2004], is the absence or presence of a current sheet (except in the case of skimming the streamer belt without crossing the current sheet). What the recognition of pseudostreamer belts provides is a new template for understanding solar wind stream structure.

[28] The new template has been a long time in coming, primarily because it was not until solar cycle 23 that higher-order fields dominated the solar magnetic configuration throughout the declining phase and into an extended minimum. During earlier cycles, especially cycle 20, the dominance of the dipolar field gave the impression that higher-order field loops clustered under the umbrella of the helmet streamer belt. Without the suppressing dipole dominance during cycle 23, higher-order field loops commonly appeared outside that umbrella, and with them, the pseudostreamer structures (as so clearly illustrated in Figure 3).

[29] In conclusion, the slow solar wind can be considerably more widely distributed throughout the heliosphere than the tilted dipole template developed for solar wind stream structure in the 1970s allows. In addition to slow wind in the streamer belt surrounding the HCS, slow wind can be found in pseudostreamer belts that, together with the streamer belt, form a global network of slow wind. This view is based upon the analysis of speed predictions from the Wang-Sheeley-Arge model, magnetic patterns derived from potential field source surface models, and spacecraft data from the ecliptic plane at 1 AU. If we identify the pseudostreamer belts with the (quasi-)separatrix layers of the separatrix-web model for the slow wind proposed by *Antiochos et al.* [2011], then the analysis provides convincing support for that model.

[30] **Acknowledgments.** The authors thank the Community Coordinated Modeling Center for providing numerous synoptic maps of the Wang-Sheeley-Arge model predictions. The authors also thank Y.-M. Wang for extensive discussions on the project and T. H. Zurbuchen for upgrading the charge-state data from the ACE spacecraft. Research for this paper was supported by the National Science Foundation under Grant AGS-0962645.

[31] The editor, Philippa Browning, would like to thank Leonard Fisk and an anonymous reviewer for their work refereeing this manuscript.

References

Antiochos, S. K., C. R. Devore, J. T. Karpen, and Z. Mikić (2007), Structure and dynamics of the Sun's open magnetic field, *Astrophys. J.*, *671*, 936–946, doi:10.1086/522489.

Antiochos, S. K., Z. Mikic, R. Lionello, V. Titov, and J. Linker (2011), A model for the sources of the slow solar wind, *Astrophys. J.*, *731*, 112–122, doi:10.1088/0004-637X/731/2/112.

Antiochos, S. K., J. Linker, R. Lionello, Z. Mikic, V. Titov, and T. H. Zurbuchen (2012), The structure and dynamics of the corona-heliosphere connection, in *Multiscale Physics in Coronal Heating and Solar Wind Acceleration*, *ISSI Space Sci. Ser.*, edited by D. Burgess et al., Springer, Dordrecht, Netherlands, in press.

Arge, C. N., J. G. Luhmann, D. Odstrcil, C. J. Schrijver, and Y. Li (2004), Stream structure and coronal sources of the solar wind during the May 12th, 1997 CME, *J. Atmos. Terr. Phys.*, *66*, 1295–1309, doi:10.1016/j.jastp.2004.03.018.

Eselevich, V. G. (1998), On the structure of coronal streamer belts, *J. Geophys. Res.*, *103*, 2021–2027, doi:10.1029/97JA02365.

Eselevich, V. G., V. G. Fainshtein, and G. V. Rudenko (1999), Study of the structure of streamer belts and chains in the solar corona, *Sol. Phys.*, *188*, 277–297, doi:10.1023/A:1005216707272.

Fisk, L. A. (2003), Acceleration of the solar wind as a result of the reconnection of open magnetic flux with coronal loops, *J. Geophys. Res.*, *108*(A4), 1157, doi:10.1029/2002JA009284.

Fisk, L. A. (2005), The open magnetic flux of the sun. I. Transport by reconnections with coronal loops, *Astrophys. J.*, *626*, 563–573, doi:10.1086/429957.

Fisk, L. A., and N. A. Schwadron (2001), The behavior of the open magnetic field of the Sun, *Astrophys. J.*, *560*, 425–438, doi:10.1086/322503.

Fisk, L. A., N. A. Schwadron, and T. H. Zurbuchen (1998), On the slow solar wind, *Space Sci. Rev.*, *86*, 51–60, doi:10.1023/A:1005015527146.

Fisk, L. A., T. H. Zurbuchen, and N. A. Schwadron (1999), On the coronal magnetic field: Consequences of large-scale motion, *Astrophys. J.*, *521*, 868–877, doi:10.1086/307556.

Gloeckler, G., et al. (1998), Investigation of the composition of solar and interstellar matter using solar wind and pickup ion measurements with SWICS and SWIMS on the ACE spacecraft, *Space Sci. Rev.*, *86*, 497–539, doi:10.1023/A:1005036131689.

Gloeckler, G., T. H. Zurbuchen, and J. Geiss (2003), Implications of the observed anticorrelation between solar wind speed and coronal electron temperature, *J. Geophys. Res.*, *108*(A4), 1158, doi:10.1029/2002JA009286.

Hundhausen, A. J. (1977), An interplanetary view of coronal holes, in *Coronal Holes and High Speed Wind Streams*, edited by J. B. Zirker, pp. 225–329, Colo. Assoc. Univ. Press, Boulder, Colo.

McComas, D. J., S. J. Bame, P. Barker, W. C. Feldman, J. L. Phillips, P. Riley, and J. W. Griffee (1998), Solar Wind Electron Proton Alpha Monitor (SWEPAM) for the Advanced Composition Explorer, *Space Sci. Rev.*, *86*, 563–612, doi:10.1023/A:1005040232597.

McComas, D. J., H. A. Elliott, and R. von Steiger (2002), Solar wind from high-latitude coronal holes at solar maximum, *Geophys. Res. Lett.*, *29*(9), 1314, doi:10.1029/2001GL013940.

Neugebauer, M., P. C. Liewer, B. E. Goldstein, X. Zhou, and J. T. Steinberg (2004), Solar wind stream interaction regions without sector boundaries, *J. Geophys. Res.*, *109*, A10102, doi:10.1029/2004JA010456.

Riley, P., and J. G. Luhmann (2012), Interplanetary signatures of unipolar streamers and the origin of the slow solar wind, *Sol. Phys.*, *277*, 355-373, doi:10.1007/s11207-011-9909-0.

Riley, P., J. A. Linker, and Z. Mikić (2001), An empirically driven global MHD model of the corona and inner heliosphere, *J. Geophys. Res.*, *106*, 15,889–15,901, doi:10.1029/2000JA000121.

Rušin, V., et al. (2010), Comparing eclipse observations of the 2008 August 1 solar corona with an MHD model prediction, *Astron. Astrophys.*, *513*, A45, doi:10.1051/0004-6361/200912778.

Smith, C. W., J. L'Heureux, N. F. Ness, M. H. Acuña, L. F. Burlaga, and J. Scheifele (1998), The ACE magnetic fields experiment, *Space Sci. Rev.*, *86*, 613–632, doi:10.1023/A:1005092216668.

Titov, V. S., Z. Mikić, J. A. Linker, R. Lionello, and S. K. Antiochos (2011), Magnetic topology of coronal hole linkages, *Astrophys. J.*, *731*, 111–125, doi:10.1088/0004-637X/731/2/111.

Wang, Y.-M., and N. R. Sheeley Jr. (1990a), Solar wind speed and coronal flux-tube expansion, *Astrophys. J.*, *355*, 726–732, doi:10.1086/168805.

Wang, Y.-M., and N. R. Sheeley Jr. (1990b), Magnetic flux transport and the sunspot-cycle evolution of coronal holes and their wind streams, *Astrophys. J.*, *365*, 372–386, doi:10.1086/169492.

Wang, Y.-M., and N. R. Sheeley Jr. (2003), The solar wind and its magnetic sources at sunspot maximum, *Astrophys. J.*, *587*, 818–822, doi:10.1086/368302.

Wang, Y.-M., N. R. Sheeley Jr., and N. B. Rich (2007), Coronal pseudostreamers, *Astrophys. J.*, *658*, 1340–1348, doi:10.1086/511416.

Wang, Y.-M., E. Robbrecht, and N. R. Sheeley Jr. (2009), On the weakening of polar magnetic fields during solar cycle 23, *Astrophys. J.*, *707*, 1372–1386.

Zhao, L., and L. Fisk (2010), Comparison of two solar minima: Narrower streamer stalk region and conserved open magnetic flux in the region outside of streamer stalk, in *SOHO-23: Understanding a Peculiar Solar Minimum*, edited by S. Cranmer, T. Hoeksema, and J. Kohl, *AIP Conf. Proc.*, *428*, 229–234.

Zhao, X. P., and D. F. Webb (2003), Source regions and storm effectiveness of frontside full halo coronal mass ejections, *J. Geophys. Res.*, *108*(A6), 1234, doi:10.1029/2002JA009606.

Zurbuchen, T. H., L. A. Fisk, G. Gloeckler, and R. von Steiger (2002), The solar wind composition throughout the solar cycle: A continuum of dynamic states, *Geophys. Res. Lett.*, *29*(9), 1352, doi:10.1029/2001GL013946.

S. K. Antiochos, NASA Goddard Space Flight Center, Greenbelt, MD 20771, USA.

N. U. Crooker, Center for Space Physics, Boston University, 725 Commonwealth Avenue, Boston, MA 02215, USA. (crooker@bu.edu)

M. Neugebauer, Lunar and Planetary Laboratory, University of Arizona, Tuscon, AZ 85721, USA.

X. Zhao, W. W. Hansen Experimental Physics Laboratory, Stanford University, Stanford, CA 94305, USA.